The Transmembrane and Cytosolic Domains of Equine Herpesvirus Type 1 Glycoprotein D Determine Golgi Retention by Regulating Vesicle Formation

Shimin Wang (smwang@xjau.edu.cn)
Xinjiang Agricultural University https://orcid.org/0000-0003-3845-1432
Xin-Rong Ren
Xinjiang Agricultural University
Qi-Ying Duan
Xinjiang Agricultural University
Lin-Hui Chen
Xinjiang Agricultural University

Research Article

Keywords: Glycoprotein D, Golgi retention, Subcellular localization, Secondary envelopment, Vesicle

Posted Date: April 21st, 2022

DOI: https://doi.org/10.21203/rs.3.rs-1538061/v1

Abstract

Accumulating evidence suggests that envelope proteins play an important role in viral secondary envelopment; however, the molecular mechanisms involved are poorly understood. To clarify these mechanisms, we studied the localization of equine herpesvirus type 1 (EHV-1) envelope proteins and found that glycoprotein D of EHV-1 (gD_{EHV-1}) was mostly retained in the Golgi complex, unlike that of HSV-1 and PRV. We used a gene truncation and replacement strategy to investigate the determinant sequence responsible for the Golgi retention phenotype and found that Golgi retention signals exhibit multi-domain features. The extracellular domain of gD_{EHV-1} (ECD_{EHV-1}) is an endoplasmic reticulum (ER)-resident domain. The transmembrane domain and cytoplasmic tail (TM-CT) of gD_{EHV-1} was found to help the protein reside in the Golgi complex. Once each of the dual domains was deleted or replaced, the mutant gD remained in the ER. $(TM\text{-}CT)_{EHV-1}$ preferentially binds to the endomembrane and induces a large number of vesicles that may originate from the Golgi complex or ER-Golgi intermediate compartment. Membrane fusion was hardly observed between the cell membrane and the induced vesicles. These findings provide further insight into the molecular mechanism underlying the Golgi retention of gD_{EHV-1}, enhancing our understanding of viral secondary envelopment.

1. Introduction

Equine herpesvirus type 1 (EHV-1) belongs to the alpha-herpesviridae subfamily, which also includes human herpesvirus type 1 (HSV-1), varicella-zoster virus, Marek's disease virus, bovine herpesvirus type 1, and pseudorabies virus (PRV)(1–5). Herpesviruses consist of four morphologically differentiable structures: a nucleoprotein core containing genomic DNA, an icosahedral capsid consisting of 162 capsomers, a proteinaceous layer of electron-dense material (tegument) augmenting the capsid, and a viral envelope as the outermost layer(6). In addition, all herpesviruses conform to the same structural plan(7). It is well known that the assembled nucleocapsid of herpesviruses in the nucleus acquires the primary envelope by budding from the inner nuclear membrane and loses it by fusing with the outer nuclear membrane to cross the nuclear membrane(8). Thereafter, the nucleocapsid coats its secondary envelope by acquiring some vesicles in the cytoplasm to form a bilayer viral particle(9). However, whether the vesicle derives from the Golgi complex or endosome remains controversial(9–14), and the mechanism of secondary envelopment in all herpesviruses remains unresolved (15, 16).

Previous studies reported that empty envelope particles without capsids, known as light particles (L-particles), form naturally in EHV-1 or other herpesvirus-infected cells(17–19), indicating that secondary envelopment proceeds in a capsid-independent manner. It is believed that herpesviruses envelope proteins play a vital role in this process. Many envelope proteins have been reported to be closely associated with secondary envelopment through interaction with teguments (i.e., UL11, UL14, UL16, UL36, UL37, UL49, and UL51) and/or capsid proteins(18, 20–27). However, data confirming the relationship between envelope proteins and secondary envelopment are limited, and the mechanism by which the envelope protein facilitates secondary envelopment is still obscure(15, 16).

The glycoprotein D (gD) envelope protein is found in almost all alpha-herpesviruses(28) and is important for secondary envelopment(25, 29, 30). Glycoprotein D encoded by some alpha-herpesviruses (i.e., HSV-1 and PRV) is a cell membrane-located protein when expressed individually, and it returns to the budding site to participate in secondary envelopment only with the help of another envelope protein, glycoprotein M (gM)(11, 25, 31–33). However, EHV-1 gD (gD_{EHV-1}) has been identified as a type of Golgi-retained protein when ectopically expressed in mammalian cells, which should be important for research on secondary envelopment(34). Although the functions of gD_{EHV-1} in facilitating virus entry have been reported, the mechanism of gD_{EHV-1} Golgi retention is still unknown. Therefore, we attempted to uncover the roles of different gD_{EHV-1} domains in this phenotype, and our results revealed that gD_{EHV-1} Golgi retention could be achieved by inhibiting vesicle formation and membrane fusion, which is regulated by its ECD and TM-CT domains.

2. Materials And Methods

2.1 Cell Culture and Treatment

BHK-21, Vero, and HeLa cells were grown in Dulbecco's modified Eagle's medium (DMEM; Hyclone Laboratories Inc, Logan, UT, USA) supplemented with 10% fetal bovine serum (FBS, Gibco™, Thermo Fisher Scientific, Waltham, MA, USA), 5 mg/mL penicillin, and 10 mg/mL streptomycin at 37°C in a humidified atmosphere of 5% CO_2. Cells were seeded in 6- or 12-well plates, and then the plasmid was transfected with lipofectamine™ 2000 reagent (Invitrogen, Groningen, Netherlands) at a confluence of 60–70% according to the manufacturer's instructions. For vesicle formation detection, cells were treated with 2.0 μM brefeldin A (BFA; Selleck Chemicals, Houston, TX, USA) for 12 h, and for the Golgi staining test, cells were treated with 0.1 mM cycloheximide (CHX; Coollaber, Beijing, China) for 3 h before proceeding with cell fixation.

2.2 Plasmids Construction

The full-length or truncated gD gene was amplified using PrimerSTAR® HS DNA polymerase (Takara, Dalian, China) from the plasmid pAcGFP-gD_{EHV-1}. The PCR product was purified using a Gel Extraction Kit (Omega Bio-Tek Inc, Norcross, VA, USA) and cloned into the pEGFP-N2 or pEGFP-C1 vector using a seamless cloning kit (Beyotime Biotechnology, Shanghai, China). The gD_{EHV-1} was fused with the "GGGGSGGGGSEQKLISEEDL" peptide at its C-terminal using PCR and cloned into a pCAGGS-MCS vector to obtain the gD-myc plasmid. The gD_{HSV-1} (GenBank: KT899744.1) and gD_{PRV} (GenBank: JQ809328.1) genes were synthesized by Sangon Biotech (Shanghai) Co., Ltd. (Shanghai, China) and cloned into the pEGFP-N2 vector. The $gD_{(TM-CT)}$ and $gD_{\Delta ECD}$ genes were synthesized and cloned into the pEGFP-C1 vector to obtain the $gD_{(TM-CT)}$-EGFP and $gD_{\Delta ECD}$-EGFP plasmids. The cloning procedure used for plasmid construction was similar, and all primers are listed in Table 1. The numbers used in the construct names denoting amino acid numbers refer to their position in the full-length gD_{EHV-1} in this study. All plasmids were confirmed by DNA sequencing.

Table 1
Primers for constructing recombinant plasmids

Plasmid name	Forward primer(5'→3')	Reverse primer(5'→3')
gD_{EHV-1}-EGFP	CTCGAGCTCAAGCTTCGAATTCGCCACCatgGctaccttcaagcttatg	GTGGCGACCGGCCGGTGGATCCCcggaagctgggtatatttaac
gD_{HSV-1}-EGFP	CTCGAGCTCAAGCTTCGAATTCGCCACCatgggggggggctgccgccagg	GTGGCGACCGGCCGGTGGATCCCgatcccgtaaaacaagggctgg
gD_{PRV}-EGFP	CTCGAGCTCAAGCTTCGAATTCGCCACCatgGtgctcgcagcgctattg	GTGGCGACCGGCCGGTGGATCCCCGGACCGGGCTGCGCTTTTAG
gD_{EHV-1}-myc	catcattttggcaaagaattcATGAGCACCTTCAAGCTGATGATGG	aaaaagatctgctagctcgagTCACAGATCCTCTTCAGAGATGAGTTTCTGC
$gD_{(1-260)}$-EGFP	GGGCTCGAGCTACCTTCAAGCTTATG	TTAggATCCACCAAgAAACCgACg
$gD_{(261-402)}$-EGFP	gggCTCgAggTgAATTCAACTTCC	TTTGGATCCCGGAAGCTGGGTATATT
$gD_{(1-36)}$-EGFP	CTCGAGCTCAAGCTTCGAATTCATGGCTACCTTCAAGCTT	GGTGGCGACCGGTGGATCCCGACGCTTGGCTTTCTCGCA
$gD_{(36-402)}$-EGFP	CTCGAGCTCAAGCTTCGAATTCATGGCGGTTCGAGGACGCCAG	GGTGGCGACCGGTGGATCCCGCGGAAGCTGGGTATATTT
$gD_{(36-348)}$-EGFP	CTCGAGCTCAAGCTTCGAATTCATGGCGGTTCGAGGACGCCAG	GGTGGCGACCGGTGGATCCCGCGTAGAGTTGCTCTTAGA
$gD_{\Delta(36-348)}$-EGFP	F1: CTCGAGCTCAAGCTTCGAATTCATGGCTACCTTCAAGCTT	R1: GACGCTGATGCCCACAAAACGCTTGGCTTTCTCGCA
	F2: TTTGTGGGCATCAGCGTC	R2: GGTGGCGACCGGTGGATCCCGCGGAAGCTGGGTATATTT
$gD_{(348-372)}$-EGFP	CTCGAGCTCAAGCTTCGAATTCATGTTTGTGGGCATCAGCGTC	GGTGGCGACCGGTGGATCCCGCAAGCAGACGTATAGAAT
$gD_{\Delta(348-372)}$-EGFP	F1: CTCGAGCTCAAGCTTCGAATTCATGGCTACCTTCAAGCTT	R1: AGTTCCTTCTTCCGACGCGTAGAGTTGCTCTTAGA
	F2: CGTCGGAAGAAGGAACT	R2: GGTGGCGACCGGTGGATCCCGCGGAAGCTGGGTATATTT
$gD_{(373-402)}$-EGFP	CTCGAGCTCAAGCTTCGAATTCATGCGTCGGAAGAAGGAACTG	GGTGGCGACCGGTGGATCCCGCGGAAGCTGGGTATATTT
$gD_{(1-372)}$-EGFP	CTCGAGCTCAAGCTTCGAATTCATGGCTACCTTCAAGCTT	GGTGGCGACCGGTGGATCCCGGACGCTGATGCCCACAAA
gD_{CH01}	F1: CTCGAGCTCAAGCTTCGAATTCTATGGGGGGGGCTGCCGCCAGG	R1: GGCGTCCTCGAACCGCTTTGCCGCGGACCCCATGGAGG
	F2: GCGGTTCGAGGACGCCAGGATAGGCCAAAGG	R2: GTTATCTAGATCCGGTGGATCCCTACGGAAGCTGGGTATATTTAAC
gD_{CH02}	F1: CTCGAGCTCAAGCTTCGAATTCTATGGGGGGGGCTGCCGCCAGG	R1: GCCCATGTTGTTCGGGGTGGCC
	F2: CCCCGAACAACATGGGCTTTGTGGGCATCAGCGTCGGTTTG	R2: GTTATCTAGATCCGGTGGATCCCTACGGAAGCTGGGTATATTTAAC
gD_{CH03}	F1: CTCGAGCTCAAGCTTCGAATTCTATGGGGGGGGCTGCCGCCAGG	R1: GGCGTCCTCGAACCGCTTTGCCGCGGACCCCATGGAGG
	F2: GCGGTTCGAGGACGCCAGGATAGGCCAAAGG	R2: CGTAGAGTTGCTCTTAGAC
	F3: GTCTAAGAGCAACTCTACGCTGATCGCCGGCGCGGTG	R3: CAGTTCCTTCTTCCGACGGTGCATCCAGTACACAAT
	F4: TTGTGTACTGGATGCACCGTCGGAAGAAGGAACTG	R4: GTTATCTAGATCCGGTGGATCCCTACGGAAGCTGGGTATATTTAAC
gD_{CH04}	F1: CTCGAGCTCAAGCTTCGAATTCTATGGGGGGGGCTGCCGCCAGG	R1: GGCGTCCTCGAACCGCTTTGCCGCGGACCCCATGGAGG
	F2: GCGGTTCGAGGACGCCAGGATAGGCCAAAGG	R2: CAAGCAGACGTATAGAAT
	F3: GGCGTCATTCTATACGTCTGCTTGCGCCGCACTCGGAAAG	R3: GTTATCTAGATCCGGTGGATCCCTACGGAAGCTGGGTATATTTAAC
gD_{CH05}	F1: CTCGAGCTCAAGCTTCGAATTCTATGGGGGGGGCTGCCGCCAGG	R1: CAGTTCCTTCTTCCGACGGTGCATCCAGTACACAAT
	F2: TTGTGTACTGGATGCACCGTCGGAAGAAGGAACTG	R2: GTTATCTAGATCCGGTGGATCCCTACGGAAGCTGGGTATATTTAAC
gD_{CH06}	F1: CTCGAGCTCAAGCTTCGAATTCTATGGGGGGGGCTGCCGCCAGG	R1: GCCCATGTTGTTCGGGGTGGCC
	F2: CCCCGAACAACATGGGCTTTGTGGGCATCAGCGTCGGTTTG	R2: CAAGCAGACGTATAGAAT
	F3: GGCGTCATTCTATACGTCTGCTTGCGCCGCACTCGGAAAG	R3: GTTATCTAGATCCGGTGGATCCCTAGATCCCGTAAAACAAGGGC
gD_{CH07}	F1: CTCGAGCTCAAGCTTCGAATTCTATGGGGGGGGCTGCCGCCAGG	R1: GGCGTCCTCGAACCGCTTTGCCGCGGACCCCATGGAGG
	F2: GCGGTTCGAGGACGCCAGGATAGGCCAAAGG	R2: CGTAGAGTTGCTCTTAGAC

Plasmid name	Forward primer(5′→3′)	Reverse primer(5′→3′)
	F3: TATGCCTTGGCGGATGCCTCTCTCAAG	R3: GTTATCTAGATCCGGTGGATCCCTAGATCCCGTAAAACAAGGGC
gD$_{CH08}$	F1: CTCGAGCTCAAGCTTCGAATTCTATGGCTACCTTCAAGCTTATGATGG	R1: CATCCGCCAAGGCATAACGCTTGGCTTTCTCGCATGTTCC
	F2: TATGCCTTGGCGGATGCCTCTCTCAAG	R2: GTTATCTAGATCCGGTGGATCCCTAGATCCCGTAAAACAAGGGC
gD$_{CH09}$	F1: CTCGAGCTCAAGCTTCGAATTCTATGGCTACCTTCAAGCTTATGATGG	R1: CATCCGCCAAGGCATAACGCTTGGCTTTCTCGCATGTTCC
	F2: TATGCCTTGGCGGATGCCTCTCTCAAG	R2: GCCCATGTTGTTCGGGGTGGCC
	F3: CCCCGAACAACATGGGCTTTGTGGGCATCAGCGTCGGTTTG	R3: GTTATCTAGATCCGGTGGATCCCTACGGAAGCTGGGTATATTTAA
gD$_{CH10}$	F1: CTCGAGCTCAAGCTTCGAATTCTATGGCTACCTTCAAGCTTATGATGG	R1: CGTAGAGTTGCTCTTAGAC
	F2: GTCTAAGAGCAACTCTACGCTGATCGCCGGCGCGGTG	R2: CAGTTCCTTCTTCCGACGGTGCATCCAGTACACAAT
	F3: TTGTGTACTGGATGCACCGTCGGAAGAAGGAACTG	R3: GTTATCTAGATCCGGTGGATCCCTACGGAAGCTGGGTATATTTAA
gD$_{CH11}$	F1: CTCGAGCTCAAGCTTCGAATTCTATGGCTACCTTCAAGCTTATGATGG	R1: CAAGCAGACGTATAGAAT
	F2: GGCGTCATTCTATACGTCTGCTTGCGCCGCACTCGGAAAG	R2: GTTATCTAGATCCGGTGGATCCCTAGATCCCGTAAAACAAGGGC
gD$_{CH12}$	F1: CTCGAGCTCAAGCTTCGAATTCTATGGCTACCTTCAAGCTTATGATGG	R1: CATCCGCCAAGGCATAACGCTTGGCTTTCTCGCATGTTCC
	F2: TATGCCTTGGCGGATGCCTCTCTCAAG	R2: CAGTTCCTTCTTCCGACGGTGCATCCAGTACACAAT
	F3: TTGTGTACTGGATGCACCGTCGGAAGAAGGAACTG	R3: GTTATCTAGATCCGGTGGATCCCTACGGAAGCTGGGTATATTTAA
gD$_{CH13}$	F1: CTCGAGCTCAAGCTTCGAATTCTATGGCTACCTTCAAGCTTATGATGG	R1: CATCCGCCAAGGCATAACGCTTGGCTTTCTCGCATGTTCC
	F2: TATGCCTTGGCGGATGCCTCTCTCAAG	R2: GCCCATGTTGTTCGGGGTGGCC
	F3: CCCCGAACAACATGGGCTTTGTGGGCATCAGCGTCGGTTTG	R3: CAAGCAGACGTATAGAAT
	F4: GGCGTCATTCTATACGTCTGCTTGCGCCGCACTCGGAAAG	R4: GTTATCTAGATCCGGTGGATCCCTAGATCCCGTAAAACAAGGGC
gD$_{CH14}$	F1: CTCGAGCTCAAGCTTCGAATTCTATGGCTACCTTCAAGCTTATGATGG	R1: CGTAGAGTTGCTCTTAGAC
	F2: TATGCCTTGGCGGATGCCTCTCTCAAG	R2: GTTATCTAGATCCGGTGGATCCCTAGATCCCGTAAAACAAGGGC

2.3 Indirect Immunofluorescence Assay

At 24 h post-transfection, cells were fixed with 4% paraformaldehyde and permeabilized with 0.1% Triton X-100 or saponin buffer (Beyotime Biotechnology) before blocking with 2% bovine serum albumin in PBS. The cells were then incubated with the specific antibody Golgi marker GP73 (F-2) or TGN38 (B-6) antibody (1:50; Santa Cruz Biotechnology Inc., Santa Cruz, TX, USA), followed by Alexa Fluor 594-labeled rabbit anti-mouse antibody (1:1,000; Thermo Fisher Scientific). The subcellular localization of live or stained cells was analyzed using an LSM510 confocal microscope (Carl Zeiss AG, Jena, Germany) with the appropriate filters. The images were analyzed using LSM Image Browser software (Carl Zeiss AG).

2.4 Cell Membrane Staining

Cells fixed with 4% paraformaldehyde were permeabilized with saponin buffer before incubating with DiI solution (1:400; Beyotime Biotechnology) for 20 min at room temperature or stained directly without permeabilization.

2.5 Transmission Electron Microscopy

The positively transfected BHK-21 cells were selected under 800 μg mL^{-1} G418. Selected cells were grown in 10-cm dishes until they reached approximately 90% confluence. The cells were then rinsed thrice with phosphate-buffered saline (PBS) before scraping and centrifuging at 300 × *g* for 10 min. The collected cells were fixed for at least 48 h in 2.5% electron microscopy-grade glutaraldehyde in 0.1 M phosphate buffer (pH 7.4) and postfixed for 60 min with 2% osmium tetroxide. Subsequently, the fixed cells were dehydrated using graded ethanol before embedding in Epon. Ultrathin sections obtained using a Leica EM UC7 Ultramicrotome (Leica Microsystems GmbH, Vienna, Austria) were stained with uranyl acetate and lead citrate. Observations were made using a Hitachi H-7500 transmission electron microscope (Hitachi, Tokyo, Japan). The number and area of vesicles were measured using ImageJ software. All data were analyzed using GraphPad Prism 8 software (GraphPad Software, San Diego, CA, USA).

3. Results

3.1 gD$_{EHV-1}$ is a type of Golgi-retained protein

A previous study showed that HSV-1 gD (gD_{HSV-1}) and PRV gD (gD_{PRV}) are cell membrane proteins(25, 35). To identify whether gD_{EHV-1} is a protein located in the cell membrane, we transfected the plasmids encoding EGFP-fused EHV-1 gD(gD_{EHV-1}), HSV-1 gD (gD_{HSV-1}), and PRV gD (gD_{PRV}) into BHK-21 cells and stained their cell membranes using DiIC18(3). Colocalization was analyzed using the Pearson's coefficient and the overlap between gD and cell membrane signal at the pixel level(36). To aid visualization, we also plotted the fluorescence intensities of different groups. The plots clearly showed that only gD_{EHV-1}-EGFP did not reached the cell membrane, indicating that transportation of gD_{EHV-1} to the cell membrane (or membrane fusion) was inhibited (Fig. 1a). Golgi retention could be observed in the majority of cells expressing gD_{EHV-1}-EGFP, differing from the gD_{HSV-1}-EGFP and gD_{PRV}-EGFP groups (Fig. 1b).

GP73, also known as Golgi phosphoprotein 2(GOLPH 2), is a type of Golgi membrane protein that primarily localizes in *cis*- and medial- Golgi, while, TGN38 is also an integral membrane protein that specifically localizes in *trans*-Golgi sub-compartments (37, 38). To further investigate the subcellular localization of the three types of glycoproteins, transfected cells were stained with GP73(F-2) or TGN38(B-6) antibody(Santa Cruz Biotechnology, USA) and treated with 0.1 mM cycloheximide (CHX) for another 3 hours to block the new protein synthesis before cell fixation, ensuring the target protein is trafficked to its final destination. In the present study, we defined the overlap of signal with that of the Golgi marker at the pixel level. The signal exceeds the Golgi marker and the stain has an edge-enhancing effect as a cell membrane protein, with no obvious edge-enhancing effect as an ER-retained protein (distributed beyond the Golgi marker, appearing reticular). Colocalization results showed that only gD_{EHV-1}-EGFP had a barely observable signal increasement beyond the signal pixel of the Golgi complex (Fig. 1c and 2a), indicating that ectopically expressed gD_{EHV-1}-EGFP could be retained in the Golgi complex in BHK-21 cells; This result was further proved by Pearson's correlation coefficient (PCC) (Fig. 1d). To ensure that the EGFP tag did not affect gD_{EHV-1} localization, the colocalization of gD_{EHV-1}-myc with Golgi marker (GP73[F-2]) in BHK-21 cells was also determined, and we did not find any differences in patterns of localization (Fig. 1c). Accordingly, these results showed that gD_{EHV-1} ,but not gD_{HSV-1} and gD_{PRV}, is a kind of Golgi-retained protein.

3.2 gD_{EHV-1} retention in Golgi Complex is a Cell Type-independent Phenotype

To verify whether gD_{EHV-1} Golgi retention of is a cell type-dependent phenotype, BHK-21, HeLa, and Vero cells were transfected with plasmids encoding gD_{EHV-1}-EGFP and EGFP. The transfected cells were fixed and stained TGN38(B-6) Golgi marker as described above. Compared with the BHK-21 cell group, considerably more trans-Golgi network derived vesicle-like structures were induced by gD_{EHV-1} in Hela and Vero cells (Fig. 2a). However, membrane fusion was thought to be inhibited because there was no significant edge-enhanced signalling. Furthermore, the PCC value and number of cells with a higher PCC value(39) were insignificant in three groups (Fig. 2b and 2c). This indicates that gD_{EHV-1} colocalized well with Golgi marker TGN38 in all three different cell types, although there was subtle difference in the localization pattern of the *trans*-Golgi network in BHK-21 cell relative to the other two cell types, attributable to cell genotype or sensitivity to CHX. Additionally, unpublished results in our lab showed that S391(located at CT domain) is phosphorylated in Hela cells but not in BHK21 cells, possibly affecting protein transportation. From these results, we concluded that gD_{EHV-1} retention in the Golgi complex is a cell type-independent phenotype. However, the mechanism by which gD_{EHV-1} is retained in the Golgi complex remains elusive.

3.3 Golgi Retention Signal (GRS) is Determined by Multiple Domains

gD_{EHV-1} is a type 1 transmembrane protein comprising four different domains, including a signal peptide (SP) (gD_{1-35}), an extracellular domain (ECD) (gD_{36-348}), a transmembrane domain (TM) ($gD_{349-372}$), and a regulatory cytoplasmic tail (CT) ($gD_{373-402}$) (Fig. 3a). To determine whether the GRS was determined by a single proper amino acid sequence, three plasmids, gD_{1-260}-EGFP, $gD_{261-402}$-EGFP, and gD_{36-402}-EGFP, were constructed and transfected into BHK-21 cells to observe their subcellular localization in live cells. The results showed that Golgi retention of all three gD_{EHV-1} truncations was completely disrupted (data not shown). We hypothesized that multiple gD_{EHV-1} domains are related to the Golgi retention phenotype.

To identify the key domains involved in Golgi retention and investigate their role thereof, eight plasmids encoding different truncations, including gD_{1-35}-EGFP (gD_{SP}-EGFP), gD_{36-402}-EGFP ($gD_{\Delta SP}$-EGFP), gD_{36-348}-EGFP (gD_{ECD}-EGFP), $gD_{\Delta(36-402)}$-EGFP ($gD_{\Delta ECD}$-EGFP), $gD_{349-372}$-EGFP (gD_{TM}-EGFP), $gD_{\Delta(349-372)}$-EGFP ($gD_{\Delta TM}$-EGFP), $gD_{373-402}$-EGFP (gD_{CT}-EGFP), and gD_{1-372}-EGFP ($gD_{\Delta CT}$-EGFP) (Fig. 3a), were constructed and transfected into BHK-21 cells. As shown in Fig. 3b, gD_{SP}-EGFP could bind to the ER-like structure in a manner characterized as saturation. Without the SP domain, $gD_{\Delta SP}$-EGFP could still be localized at an unknown intracellular membrane but not at the cell membrane, indicating that another binding site in $gD_{(36-402)}$ for some internal membranes exists. The fusion protein gD_{ECD}-EGFP was distributed evenly in the cytoplasm, while a large number of $gD_{\Delta ECD}$-EGFP was trafficked to the membrane and partly formed secreted vesicles in the extracellular space. In the present study, gD_{TM}-EGFP localization was characterized by membrane tropism in accordance with the hydrophobic transmembrane domain. A substantial percentage of the TM-defective mutant protein $gD_{\Delta TM}$-EGFP accumulated in the cytoplasm and some of it was located in the cell membrane. EGFP fused with the CT domain is mainly secreted out of the cell, while $gD_{\Delta CT}$-EGFP is retained in the ER, revealing the important role of the CT domain in protein trafficking. In all the groups mentioned above, only the findings on $gD_{\Delta TM}$-EGFP seemed to be inconsistent with those on $gD_{\Delta CT}$-EGFP. It was anticipated that localization between the $gD_{\Delta TM}$-EGFP and $gD_{\Delta CT}$-EGFP groups would be similar because deletion of the TM domain may cause the translocation of the CT domain from the cytoplasm to the endomembrane lumen, leading to the latter losing its regulatory function. A possible explanation for this inconsistency is that translocated CT could bind directly to ECD in the endomembrane lumen and affect the normal conformation of ECD, causing $gD_{\Delta TM}$-EGFP to become a secreted protein. Collectively, these results showed that all mutant gD could not salvage the Golgi retention phenotype, and it was confirmed that Golgi localization of gD_{EHV-1} was determined by the combination of its multiple domains.

3.4 Localization Test of Two-Domain Combination

To ensure the function of each gD_{EHV-1} domain, we continued to identify the localization of every two adjacent domains. Three plasmids encoding $gD_{(SP-ECD)}$-EGFP, $gD_{(ECD-TM)}$-EGFP, and $gD_{(TM-CT)}$-EGFP were constructed and transfected into BHK-21 cells (Fig. 4a). Localization of the truncated proteins was observed following the same steps described above. The results showed that $gD_{(SP-ECD)}$-EGFP is retained in the ER structure, indicating that the ER retention phenotype of the gD_{EHV-1} mutant or its chimeric form is TM-CT domain-independent. The $gD_{(ECD-TM)}$-EGFP was primarily located in the cell membrane and inner membrane-related structures, in accordance with the fusion protein gD_{TM}-EGFP. $gD_{(TM-CT)}$-EGFP is preferentially localized at the inner membrane rather than the cell membrane (Fig. 4b). A likely reason for the susceptibility of the TM-CT peptide to localization in the inner membrane rather than the cell membrane is the existence of double KKXX ER retrieval motifs in the TM-CT domain. Additionally, many vesicles in the cytoplasm but not in the cell membrane were induced by $gD_{(TM-CT)}$-EGFP. Fusion between vesicles and the cell membrane was hardly observed, suggesting that the TM-CT domain may also inhibit the fusion process (Fig. 4b). These consistent results not only further proved the reliability of our conclusions but also provided some new insights into Golgi retention.

3.5 TM-CT Domain of gD_{EHV-1} Should be a Vesicle Inducing Sequence

Vesicle traffic is the main pathway in cells for membrane protein transportation and is important for intercellular communication. To determine whether the punctate structures induced by $gD_{(TM-CT)}$ and $gD_{(SP-TM-CT)}$ comprised empty vesicles or solid granules, BHK-21 cells were transfected with $gD_{(SP-TM-CT)}$-EGFP ($gD_{\Delta ECD}$-EGFP), $gD_{(TM-CT)}$-EGFP, and empty vector, or were mock-transfected and selected using G418. Cells were fixed using 2.5% glutaraldehyde and observed using transmission electron microscopy (TEM). The results showed that both $gD_{\Delta ECD}$-EGFP and $gD_{(TM-CT)}$-EGFP induced considerably more vesicles than the control group. The vesicles induced by $gD_{(TM-CT)}$-EGFP primarily accumulated in the cytoplasm (cytoplasmic vesicle, CV), while those induced by $gD_{\Delta ECD}$-EGFP were susceptible to secretion out of cells (secreted vesicle, SV). Mock-transfected cell-induced vesicles were detected both intracellularly and extracellularly (natural vesicle, NV). The mean diameter of CV was approximately 95 nm, approximately half the size of SV and NV (Fig. 5a–c).

Cargo vesicles budding from ER exit sites (ERES) assemble into the ER-Golgi intermediate compartment (ERGIC) to complete ER–Golgi transportation (40–42). A chemical compound, brefeldin A (BFA), can disrupt the ERGIC and Golgi complex to block this process (43). In the present study, vesicle formation induced by $gD_{(TM-CT)}$-EGFP or $gD_{\Delta ECD}$-EGFP could be inhibited by BFA treatment (Fig. 5d), indicating that the induced vesicles originated from either the ER-Golgi intermediate compartment (ERGIC) or Golgi complex. These results suggested that $(TM\text{-}CT)_{EHV-1}$ should be a vesicle-inducing sequence, which could induce vesicles from the Golgi complex or ERGIC.

3.6 TM-CT Domain Regulated Golgi retention of gD_{EHV-1}

gD_{EHV-1} and gD_{HSV-1} are homologous proteins with similar domains (Fig. 6a). Ectopically expressed gD_{HSV-1} could be transported to the cell membrane, while a large number of gD_{EHV-1} were distributed in the Golgi complex. To further assess the function of each domain, we constructed a series of chimeric gD(gD_{Ch}) genes (Fig. 6b) between gD_{EHV-1} and gD_{HSV-1} using the seamless DNA cloning method and transfected them into BHK-21 cells. Cells were transfected with the chimeric plasmids were incubated with CHX for 3 h, 24 h after transfection, then fixed and stained with Golgi marker GP73 (F-2) antibody. Colocalization was analysed as described above. To aid visualization, we also plotted the fluorescence intensity of different groups, and results showed that several chimeric proteins primarily overlapped with the Golgi complex, including gD_{Ch01}, gD_{Ch02}, and gD_{Ch09}, all containing both TM_{EHV-1} and CT_{EHV-1} domains. Some were located on the cell membrane, including gD_{Ch05}, gD_{Ch06}, gD_{Ch08}, gD_{Ch12}, and gD_{Ch13}, which combine ECD_{HSV-1} and non-$(TM\text{-}CT)_{EHV-1}$. Six chimeric proteins, gD_{Ch03}, gD_{Ch04}, gD_{Ch07}, gD_{Ch10}, gD_{Ch11}, and gD_{Ch14}, have ECD_{EHV-1} and non-$(TM\text{-}CT)_{EHV-1}$ as a common feature. The localization of these six chimeric proteins does not fit well with the Golgi complex, and the pattern of localization seems similar to that in cells treated with Brefeldin A (BFA), indicating that these proteins should be localized in the ER. From these results, we concluded that ECD_{EHV-1} (gD_{Ch03}, gD_{Ch04}, gD_{Ch10}, and gD_{Ch11}) but not ECD_{HSV-1} (gD_{Ch05}, gD_{Ch06}, gD_{Ch08}, gD_{Ch12}, and gD_{Ch13}) bears an ER-resident signal, which is transported to the Golgi complex only with the help of the $(TM\text{-}CT)_{EHV-1}$ domain (gD_{Ch01}, gD_{Ch03}, gD_{Ch04}, gD_{Ch07}, gD_{Ch10}, gD_{Ch11}, and gD_{Ch14}). The function of the $(TM\text{-}CT)_{EHV-1}$ domain was lost once any part was replaced by an analogous sequence from other transmembrane proteins (gD_{Ch02}, gD_{Ch05}, gD_{Ch06}, gD_{Ch12}, and gD_{Ch13}). On the other hand, the chimeric protein-containing the $(TM\text{-}CT)_{EHV-1}$ domain could hardly be detected on the cell membrane, indicating that $(TM\text{-}CT)_{EHV-1}$ could also inhibit protein trafficking from the Golgi complex to the cell membrane (gD_{Ch01}, gD_{Ch02}, and gD_{Ch09}) (Fig. 6c). Collectively, Golgi retention of the gD mutant and its chimeric form could be rescued by the $(TM\text{-}CT)_{EHV-1}$ domain by facilitating ER–Golgi trafficking and inhibiting transportation to the cell membrane (Fig. 7).

4. Discussion

Membrane traffic during virus egress involves a set of highly dynamic and interrelated compartments, which rapidly transport proteins and change their localization(10, 44–46). All viral proteins are transported to their destinations, either independently or as a complex. This may be the reason why controversies regarding the localization of single envelope proteins using different methods have erupted(47–50). The target membrane protein travels one or more steps of its journey without an additional partner, which also helps us elucidate the whole journey, including secondary envelopment. The envelope protein gD encoded by some *α*-herpesvirus (i.e., HSV-1 and PRV) is cell membrane-located when expressed individually and is completely unable to localize at the site of secondary envelopment(11, 25, 31, 32, 35). Accordingly, it seems unsuitable to reveal the secondary envelopment process through the ectopic expression of envelope proteins. Unlike in other *α*-herpesviruses, ectopically expressed gD_{EHV-1} is retained in the Golgi complex, which is associated with the secondary envelopment process(34). Although a previous study showed that gD_{EHV-1} was detected on the cell membrane of CHO and RK13 cells, very weak fluorescence on the cell membrane and strong signals in the cytoplasm were detected, also indirectly proving the Golgi retention phenotype of $gD_{EHV-1(51)}$. The present study demonstrated that gD_{EHV-1} Golgi retention might be achieved by inhibiting vesicle formation, which is mainly regulated by its TM-CT domain. Although our results lack comprehensive information on the mechanism of gD_{EHV-1} Golgi retention, they help us better understand secondary envelopment.

Golgi localization of cellular proteins is thought to be related to retrieval and/or retention processes(52). Retrieval of resident Golgi proteins from distal compartments is largely dependent on the signals within the sequence located in the cytosolic domains. Golgi retention refers to the process by which Golgi-resident proteins are prevented from being transported to distal compartments. Unlike retrieval signals, retention signals are more complex and usually involve luminal, transmembrane, and multimerization domains(53–55). Subcellular localization results suggested that Golgi retention of gD_{EHV-1} was determined by multiple domains. The $(TM\text{-}CT)_{EHV-1}$ domain could facilitate the transportation of both ER-resident and non-ER-resident proteins from the ER to the Golgi complex. The transported protein is retained in the Golgi complex through inhibition of vesicle formation induced by the $(TM\text{-}CT)_{EHV-1}$ domain. Vesicle formation is likely controlled by phosphorylation modification of the CT domain, which is regulated by oligomerization/de-oligomerization of the TM-CT domain through the luminal ECD domain. Different binding proteins or ECD modification may occur in the lumen of ER and Golgi complex to regulate the oligomerization/de-oligomerization of gD (56). Only the CT_{EHV-1} oligomer (or phosphorylation) can recruit host proteins to induce vesicle formation (57). Finally, even if vesicles form, membrane fusion with the cell membrane would be inhibited.

Viruses have evolved numerous mechanisms to ensure that structural proteins are present at budding sites. Most enveloped viruses acquire their envelope and bud from the plasma membrane, while some, like herpesviruses, utilize inner membranes for assembly (58). Glycoprotein D encoded by HSV-1 and PRV can be relocated to the Golgi complex from the cell membrane using gM (11, 25, 31, 32). Glycoprotein B (gB) of HSV-1 can be transported from the cell membrane to the *trans*-Golgi network through the mediation of two motifs, YTQV and LL, in the cytosolic tail (59). The Golgi-residency of gpI (gE) encoded by VZV is also determined by two motifs in the cytosolic tail, an AYRV signal sequence, and a C-terminal sequence (60). HSV-1 gE and its homologs have endocytic targeting motifs that direct the protein from the cytoplasmic membrane to the endosome or Golgi complex (61). Although a similar tyrosine motif also exists in the cytosolic tail of gD_{EHV-1}, Golgi-retention can only be realized by the combination of the TM and CT domains, indicating that the Golgi retention mechanism is not solely dependent on the TM domain (62).

In summary, our data demonstrate that a multi-domain-based sorting mechanism mediates the Golgi retention of gD_{EHV-1} in BHK-21 cells. The discovered mechanism is dissimilar to that reported previously for other glycoproteins. Our model proposes that ER-resident ECD_{EHV-1} is transported to the Golgi complex with the help of the $(TM\text{-}CT)_{EHV-1}$ domain, while further transportation is restrained by the inhibition of vesicle formation and membrane fusion. These findings provide further insight into the molecular mechanism of Golgi retention in gD_{EHV-1} and may enhance our understanding of the secondary envelopment process.

Declarations

Conflict of Interest The authors declare that they have no conflict of interest.

Funding This work was supported by grants from the National Natural Science Foundation of China (31860710); Xinjiang Uygur Autonomous Region Natural Fund (2018D01B17) from Science and Technology Department of Xinjiang Uygur Autonomous Region, China.

Ethical Approval Not applicable

Consent to Publish Not applicable

Authors' contributions S.-M. Wang conceived and designed the experiments. S.-M. Wang, X.-R. Ren, Q.-Y. Duan and L.-H. Chen performed the experiments. S.-M. Wang analyzed the data and wrote the manuscript. All authors read and approved the final manuscript.

Competing Interests The authors declare that they have no competing financial interests.

Availability of data and materials All data generated or analyzed during this study are included in this published article.

Acknowledgement The authors would like to thank Dr. Shi-Qiang Wang at University of Limerick for his proof reading and language polishing.

ORCID

Shi-Min Wang https://orcid.org/0000-0003-3845-1432

References

1. Shahin F, Raza S, Yang K, Hu C, Chen Y, Chen H, Guo A (2017) Bovine herpesvirus 1 tegument protein UL21 plays critical roles in viral secondary envelopment and cell-to-cell spreading. Oncotarget 8(55):94462–94480
2. Ortiz DA, Glassbrook JE, Pellett PE (2016) Protein-Protein Interactions Suggest Novel Activities of Human Cytomegalovirus Tegument Protein pUL103. J Virol 90(17):7798–7810
3. Yang L, Wang M, Cheng A, Yang Q, Wu Y, Jia R, Liu M, Zhu D, Chen S, Zhang S (2019) Innate immune evasion of alphaherpesvirus tegument proteins. Front Immunol 10:2196
4. Schvartz G, Edery N, Moss L, Hadad R, Steinman A, Karniely S (2020) Equid Herpesvirus 8 Isolated From an Adult Donkey in Israel.Journal of Equine Veterinary Science; 94
5. Radalj A, Milic N, Stevanovic O, Veljovic L, Nisavic J (2021) Genetic Characterization of Equine Herpesvirus 1 from Clinical Cases and Asymptomatic Horses in Serbia and Bosnia and Herzegovina. Pakistan Veterinary Journal 41(4):567–573
6. Brack AR, Klupp BG, Granzow H, Tirabassi R, Mettenleiter TC (2000) Role of the Cytoplasmic Tail of Pseudorabies Virus Glycoprotein E in Virion Formation. J Virol 74(9):4004–4016
7. Póka N, Csabai Z, Pásti E, Tombácz D, Boldogkői Z (2017) Deletion of the us7 and us8 genes of pseudorabies virus exerts a differential effect on the expression of early and late viral genes. Virus Genes 53(9):1–10

8. Zhang K, Brownlie R, van Snider M, Hurk S (2016) Phosphorylation of bovine herpesvirus 1 VP8 plays a role in viral DNA encapsidation and is essential for its cytoplasmic localization and optimal virion incorporation. J Virol 90(9):4427–4440
9. Mettenleiter TC (2004) Budding events in herpesvirus morphogenesis. Virus Res 106(2):167–180
10. Owen DJ, Crump CM, Graham SC (2015) Tegument assembly and secondary envelopment of alphaherpesviruses. Viruses 7(9):5084–5114
11. Hollinshead M, Johns HL, Sayers CL, Gonzalez-Lopez C, Smith GL, Elliott G (2012) Endocytic tubules regulated by Rab GTPases 5 and 11 are used for envelopment of herpes simplex virus. EMBO J 31(21):4204–4220
12. Meckes DG Jr, Marsh JA, Wills JW (2010) Complex mechanisms for the packaging of the UL16 tegument protein into herpes simplex virus. Virology 398(2):208–213
13. Turcotte S, Letellier J, Lippé R (2005) Herpes simplex virus type 1 capsids transit by the trans-Golgi network, where viral glycoproteins accumulate independently of capsid egress. J Virol 79(14):8847–8860
14. Sugimoto K, Uema M, Sagara H, Tanaka M, Sata T, Hashimoto Y, Kawaguchi Y (2008) Simultaneous tracking of capsid, tegument, and envelope protein localization in living cells infected with triply fluorescent herpes simplex virus 1. J Virol 82(11):5198–5211
15. Poorebrahim M, Salarian A, Najafi S, Abazari MF, Aleagha MN, Dadras MN, Jazayeri SM, Ataei A, Poortahmasebi V (2017) Regulatory network analysis of Epstein-Barr virus identifies functional modules and hub genes involved in infectious mononucleosis. Arch Virol 162(5):1299–1309
16. Varsani A, Frankfurter G, Stainton D, Male MF, Kraberger S, Burns JM (2017) Identification of a polyomavirus in Weddell seal (Leptonychotes weddellii) from the Ross Sea (Antarctica). Arch Virol 162(5):1403–1407
17. Azmi MLM, Field HJ, Rixon F, Mclauchlan J (2002) Protective immune responses induced by non-infectious L-particles of equine herpesvirus type-1: Implication of cellular immunity. J Microbiol 40(1):341–368
18. Oda S, Arii J, Koyanagi N, Kato A, Kawaguchi Y (2016) The interaction between herpes simplex virus 1 tegument proteins UL51 and UL14 and its role in virion morphogenesis. J Virol 90(19):8754–8767
19. Rixon F, Addison C, McLauchlan J (1992) Assembly of enveloped tegument structures (L particles) can occur independently of virion maturation in herpes simplex virus type 1-infected cells. J Gen Virol 73(2):277–284
20. Desai P, Sexton GL, McCaffery JM, Person S (2001) A null mutation in the gene encoding the herpes simplex virus type 1 UL37 polypeptide abrogates virus maturation. J Virol 75(21):10259–10271
21. Desai PJ (2000) A null mutation in the UL36 gene of herpes simplex virus type 1 results in accumulation of unenveloped DNA-filled capsids in the cytoplasm of infected cells. J Virol 74(24):11608–11618
22. Baines JD, Roizman B (1992) The UL11 gene of herpes simplex virus 1 encodes a function that facilitates nucleocapsid envelopment and egress from cells. J Virol 66(8):5168–5174
23. Starkey JL, Han J, Chadha P, Marsh JA, Wills JW (2014) Elucidation of the block to herpes simplex virus egress in the absence of tegument protein UL16 reveals a novel interaction with VP22. J Virol 88(1):110–119
24. Farnsworth A, Wisner TW, Johnson DC (2007) Cytoplasmic residues of herpes simplex virus glycoprotein gE required for secondary envelopment and binding of tegument proteins VP22 and UL11 to gE and gD. J Virol 81(1):319–331
25. Arii J, Shindo K, Koyanagi N, Kato A, Kawaguchi Y (2016) Multiple roles of the cytoplasmic domain of herpes simplex virus 1 envelope glycoprotein D in infected cells. J Virol 90(22):10170–10181
26. Liu T, Wang M, Cheng A, Jia R, Yang Q, Wu Y, Liu M, Zhao X, Chen S, Zhang S, Zhu D, Tian B, Rehman MU, Liu Y, Yu Y et al (2020) Duck plague virus gE serves essential functions during the virion final envelopment through influence capsids budding into the cytoplasmic vesicles. Sci Rep 10(1):1–9
27. Wilson DW, Motor, Skills (2021) Recruitment of Kinesins, Myosins and Dynein during Assembly and Egress of Alphaherpesviruses. Viruses-Basel 13(8):1622
28. Connolly SA, Jackson JO, Jardetzky TS, Longnecker R (2011) Fusing structure and function: a structural view of the herpesvirus entry machinery. Nat Rev Microbiol 9(5):369–381
29. Johnson DC, Wisner TW, Wright CC (2011) Herpes simplex virus glycoproteins gB and gD function in a redundant fashion to promote secondary envelopment. J Virol 85(10):4910–4926
30. Farnsworth A, Goldsmith K, Johnson DC (2003) Herpes simplex virus glycoproteins gD and gE/gI serve essential but redundant functions during acquisition of the virion envelope in the cytoplasm. J Virol 77(15):8481–8494
31. Crump CM, Bruun B, Bell S, Pomeranz LE, Minson T, Browne HM (2004) Alphaherpesvirus glycoprotein M causes the relocalization of plasma membrane proteins. J Gen Virol 85(12):3517–3527
32. Lau S-YK, Crump CM (2015) HSV-1 gM and the gK/pUL20 complex are important for the localization of gD and gH/L to viral assembly sites. Viruses 7(3):915–938
33. Li C, Wang M, Cheng A, Jia R, Yang Q, Wu Y, Zhu D, Zhao X, Chen S, Liu M, Zhang S, Ou X, Mao S, Gao Q, Sun D et al (2021) The Roles of Envelope Glycoprotein M in the Life Cycle of Some Alphaherpesviruses. Front Microbiol 12:631523
34. Wang S, Zhang Y, Hu Y, Su Y, Ran D, Bao X (2016) Impact of fluorescent protein tag on gD envelope protein subcellular localization in BHK-21 cells. Wei sheng wu xue bao = Acta microbiologica Sinica 56(7):1194–1201
35. Whiteley A, Bruun B, Minson T, Browne H (1999) Effects of targeting herpes simplex virus type 1 gD to the endoplasmic reticulum and trans-Golgi network. J Virol 73(11):9515–9520

36. Talamas-Lara D, Acosta-Virgen K, Chavez-Munguia B, Lagunes-Guillen A, Salazar-Villatoro L, Espinosa-Cantellano M, Martinez-Palomo A Golgi apparatus components in Entamoeba histolytica and Entamoeba dispar after monensin treatment.Microscopy Research and Technique2021:1887–1896
37. Kladney RD, Bulla GA, Guo L, Mason AL, Tollefson AE, Simon DJ, Koutoubi Z, Fimmel CJ (2000) GP73, a novel Golgi-localized protein upregulated by viral infection. Gene 249(1–2):53–65
38. Luzio JP, Brake B, Banting G, Howell KE, Braghetta P, Stanley KK (1990) Identification, sequencing and expression of an integral membrane protein of the trans-Golgi network (TGN38). Biochem J 270(1):97–102
39. Bolte S, Cordelières F (2010) A guided tour into subcellular colocalization analysis in light microscopy. J Microsc 224(3):213–232
40. Matsui Y, Hirata Y, Wada I, Hosokawa N (2020) Visualization of procollagen IV reveals ER-to-Golgi transport by ERGIC-independent carriers. Cell Struct Funct 45(2):107–119
41. Hanada K (2020) Organelle contacts: Sub-organelle zones to facilitate rapid and accurate inter-organelle trafficking of lipids. Traffic 21(1):189–196
42. Gomez-Navarro N, Melero A, Li X-H, Boulanger J, Kukulski W, Miller EA (2020) Cargo crowding contributes to sorting stringency in COPII vesicles. J Cell Biol 219(7):e201806038
43. Fujiwara T, Oda K, Yokota S, Takatsuki A, Ikehara Y (1988) Brefeldin A causes disassembly of the Golgi complex and accumulation of secretory proteins in the endoplasmic reticulum. J Biol Chem 263(34):18545–18552
44. Omari S, Makareeva E, Gorrell L, Jarnik M, Lippincott-Schwartz J, Leikin S (2020) Mechanisms of procollagen and HSP47 sorting during ER-to-Golgi trafficking.Matrix biology: journal of the International Society for Matrix Biology:79–94
45. Lazaro-Dieguez F, Musch A (2020) Low Rho activity in hepatocytes prevents apical from basolateral cargo separation during trans-Golgi network to surface transport. Traffic 21(5):364–374
46. Treyer A, Pujato M, Pechuan X, Musch A (2016) Iterative sorting of apical and basolateral cargo in Madin-Darby canine kidney cells. Mol Biol Cell 27(14):2259–2271
47. Flowers CC, Flowers SP, Jennings SR, O'Callaghan DJ, Virology (1995) ; 208(1):9–18
48. Munro K, Wellington J, Love D, Whalley J (1999) Characteristics of glycoprotein B of equine herpesvirus 1 expressed by a recombinant baculovirus. Vet Microbiol 68(1–2):49–57
49. Osterrieder N, Wagner R, Brandmüller C, Schmidt P, Wolf H, Kaaden O-R (1995) Protection against EHV-1 challenge infection in the murine model after vaccination with various formulations of recombinant glycoprotein gp14 (gB). Virology 208(2):500–510
50. Love D, Bell C, Pye D, Edwards S, Hayden M, Lawrence G, Boyle D, Pye T, Whalley J (1993) Expression of equine herpesvirus 1 glycoprotein D by using a recombinant baculovirus. J Virol 67(11):6820–6823
51. Wellington J, Lawrence G, Love D, Whalley J (1996) Expression and characterization of equine herpesvirus 1 glycoprotein D in mammalian cell lines. Arch Virol 141(9):1785–1793
52. Gerrard SR, Nichol ST (2002) Characterization of the Golgi retention motif of Rift Valley fever virus GN glycoprotein. J Virol 76(23):12200–12210
53. Opat AS, van Vliet C, Gleeson PA (2001) Trafficking and localisation of resident Golgi glycosylation enzymes. Biochimie 83(8):763–773
54. Munro S (1998) Localization of proteins to the Golgi apparatus. Trends Cell Biol 8(1):11–15
55. Gleeson PA (1998) Targeting of proteins to the Golgi apparatus. Histochem Cell Biol 109(5):517–532
56. Sun X, Tie HC, Chen B, Lu L (2020) Glycans function as a Golgi export signal to promote the constitutive exocytic trafficking. J Biol Chem 295(43):14750–14762
57. Danielli L, Li X, Tuler T, Daniel R (2020) Quantifying the distribution of protein oligomerization degree reflects cellular information capacity. Sci Rep 10(1):17689
58. Schaecher SR, Diamond MS, Pekosz A (2008) The transmembrane domain of the severe acute respiratory syndrome coronavirus ORF7b protein is necessary and sufficient for its retention in the Golgi complex. J Virol 82(19):9477–9491
59. de Beitia Ortiz I, Cantero-Aguilar L, Longo M, Berlioz-Torrent C, Rozenberg F (2007) Contribution of endocytic motifs in the cytoplasmic tail of herpes simplex virus type 1 glycoprotein B to virus replication and cell-cell fusion. J Virol 81(24):13889–13903
60. Zhu Z, Hao Y, Gershon MD, Ambron RT, Gershon AA (1996) Targeting of glycoprotein I (gE) of varicella-zoster virus to the trans-Golgi network by an AYRV sequence and an acidic amino acid-rich patch in the cytosolic domain of the molecule. J Virol 70(10):6563–6575
61. Alconada A, Bauer U, Sodeik B, Hoflack B (1999) Intracellular traffic of herpes simplex virus glycoprotein gE: characterization of the sorting signals required for its trans-Golgi network localization. J Virol 73(1):377–387
62. Welch LG, Munro S (2019) A tale of short tails, through thick and thin: investigating the sorting mechanisms of Golgi enzymes. FEBS Lett 593(17):2452–2465

Figures

Figure 1

gD_{EHV-1} could not be transported to the cell membrane and should therefore be a Golgi-retained protein. (a) Representative images of gD_{EHV-1}-EGFP, gD_{HSV-1}-EGFP, gD_{PRV}-EGFP or EGFP co-labelling with DiIC18(3) in BHK-21 cells and plots of pixel intensity along the white lines in their left merged images. (b) Number of cells that could be detected by gD_{EHV-1}-EGFP, gD_{HSV-1}-EGFP, gD_{PRV}-EGFP or EGFP in the cell membrane. The number of cell-expressing target proteins was determined in four independent experiments (n=30 cells). (c) Representative images of gD_{EHV-1}-EGFP, gD_{HSV-1}-EGFP, gD_{PRV}-EGFP or EGFP co-labelling with Golgi marker GP73(F-2) in BHK-21 cells and plots of pixel intensity along white line in their left merged images. (d) Quantification of colocalization between gD_{EHV-1}-EGFP or gD_{HSV-1}-EGFP or gD_{PRV}-EGFP or EGFP and GP73 in BHK-21 cells (n = 30 cells). Different lowercase letters indicate significant differences between each group. Data are shown as mean ± SEM. Differences were considered statistically significant when $p < 0.05$ (*$p < 0.05$, **$p < 0.01$, ****$p < 10^{-5}$; ns, not significant). Nuclei were stained with DAPI. Bar = 10 μm.

Figure 2

Retention of gD_{EHV-1} in the Golgi complex is a cell type-independent phenotype.

(a) Representative images of gD_{EHV-1}-EGFP or EGFP co-labeling with Golgi marker TGN38(B-6) in BHK-21, Hela, Vero cells and plots of pixel intensity along the white lines in their top merged images. Nuclei were stained with DAPI. Bar = 10 μm. (b) Quantification of colocalization between gD_{EHV-1}-EGFP or EGFP and TGN38 in BHK-21, Hela, or Vero cells (*n* = 30 cells). (c) Number of cells whose PCC value between gD and TGN38 is greater than 0.6. Different lowercase letters indicate significant differences between each group. Data are shown as mean ± SEM. *p* values were considered significant when $p < 0.05$ and are denoted as *$p < 0.05$, **$p < 0.01$, ****$p < 10^{-5}$; ns, not significant.

Figure 3

Distribution characterization of gD_{EHV-1} truncations in BHK-21 cells

(a) Diagram of the complete sequence of gD_{EHV-1}-EGFP and the eight different truncations. (b) Subcellular localization of EGFP-tagged full-length gD_{EHV-1} and its truncations. BHK-21 cells transfected with gD_{EHV-1} and its truncations were observed using a live-cell imaging method at 24 h post-transfection. This experiment was repeated independently twice, with similar results obtained each time. Bar = 10 μm.

Figure 4

Subcellular localization of two-domain combination

(a) Schematic representation of full-length gD and two-domain combinations. (b) Representative images of $gD_{(SP-ECD)}$-EGFP, $gD_{(ECD-TM)}$-EGFP, and $gD_{(TM-CT)}$-EGFP. BHK-21 cells transfected with $gD_{(SP-ECD)}$-EGFP, $gD_{(ECD-TM)}$-EGFP, and $gD_{(TM-CT)}$-EGFP were observed 24 h post-transfection using laser scanning microscopy. This experiment was repeated independently twice, and comparable results were obtained each time. Bars = 10 μm.

Figure 5

Characterization of vesicles induced by $gD_{(TM-CT)}$ and $gD_{\Delta ECD}$.

(a) Representative TEM images of vesicles induced by $gD_{(TM-CT)}$ and $gD_{\Delta ECD}$. BHK-21 cells transfected with plasmids $gD_{(TM-CT)}$-EGFP, $gD_{\Delta ECD}$-EGFP, and empty vector or mock-transfected were fixed and processed for TEM at about 90% confluence. The images show that plasmid $gD_{\Delta ECD}$-EGFP could induce both secreted vesicles (long arrows) and multivesicular bodies (short arrows) while plasmid $gD_{(TM-CT)}$-EGFP could mainly induce cytoplasmic vesicles (CV). Fewer vesicles were observed in the empty vector and mock-transfected groups. Mitochondria are indicated by black asterisks. Nu, nuclear. (b−c) The number and size of vesicles (*n* = 15 cells) were analysed using ImageJ and GraphPad Prism 8. (d) Representative images of vesicle formation inhibition by BFA. BHK-21 cells expressing $gD_{(TM-CT)}$-EGFP, $gD_{\Delta ECD}$-EGFP, or EGFP were treated with BFA for 12 h before fixation, then stained with DiIC18 (3) and observed using laser scanning microscopy. Data are shown as mean ± SEM. *p* values were considered significant when $p < 0.05$ and denoted as *$p < 0.05$, **$p < 0.01$, ****$p < 10^{-5}$; ns, not significant.

Figure 6

Sequence homology analysis of gD_{EHV-1} and gD_{HSV-1} and subcellular localization of a series of gD_{ch} proteins.

(a) Alignment between the gD of EHV-1 and HSV-1 using Blastp. The signal peptide is coloured pink, and the transmembrane region is coloured blue. Identical residues are marked with red boxes and equivalent residues with white boxes. (b) Schematic representation of full-length gD_{EHV-1} and gD_{HSV-1} and chimeric gDs. (c) Subcellular localization of chimeric gD. BHK-21 cells were transfected with the plasmid encoding chimeric gDs for 24 h. The cells were fixed and stained with anti-TGN38(B-6) monoantibody and DAPI. Merged pictures showed that gD_{Ch01}, gD_{Ch02}, and gD_{Ch09} fitted well with the Golgi complex, indicating that these chimeric proteins were Golgi-retained. gD_{Ch05}, gD_{Ch06}, gD_{Ch08}, gD_{Ch12}, and gD_{Ch13} could be transported to the cell membrane, and gD_{Ch03}, gD_{Ch04}, gD_{Ch07}, gD_{Ch10}, gD_{Ch11}, and gD_{Ch14} were retained in the ER. This experiment was repeated independently twice, with similar results obtained each time. Bar = 10 μm.

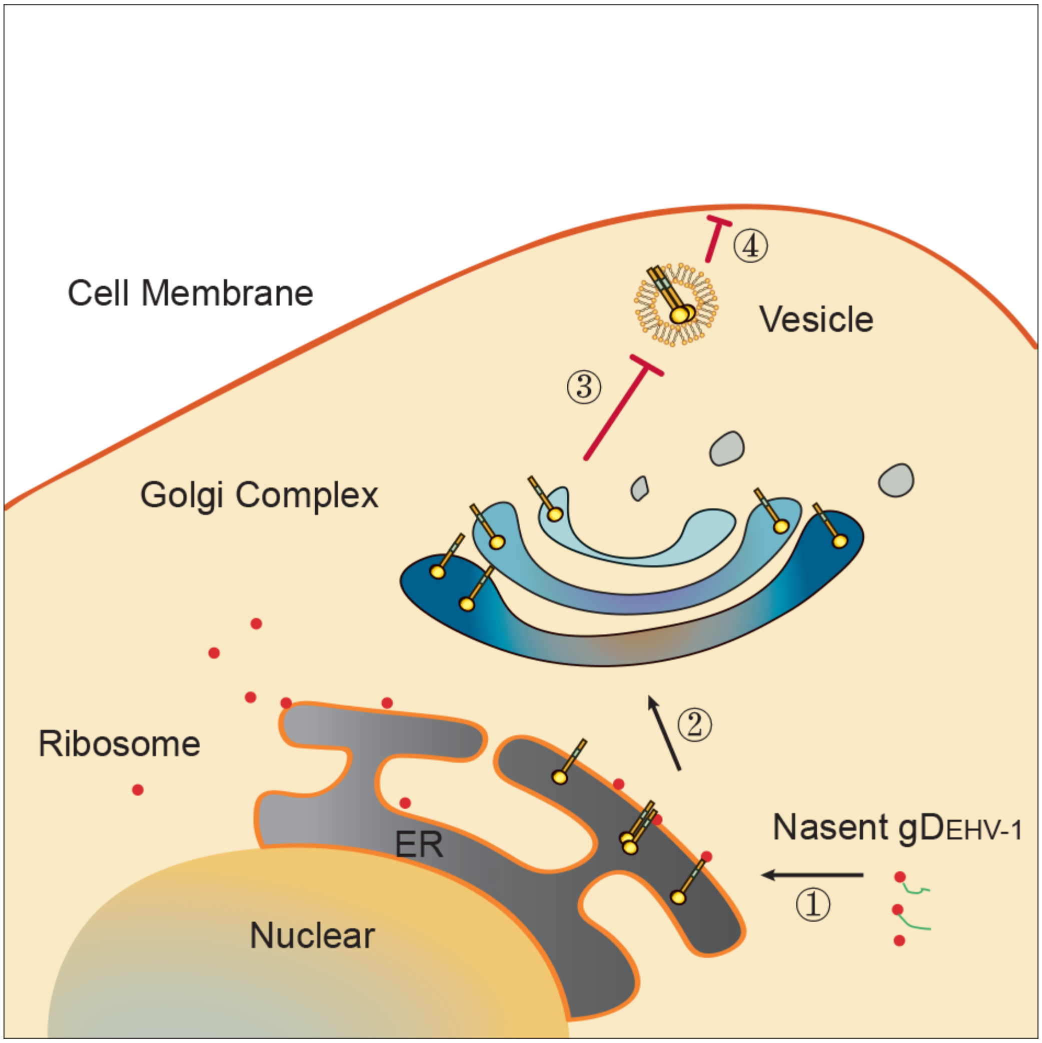

Figure 7

A model was proposed to illustrate the link between Golgi retention and each domain. The gD signal peptide was synthesized by ribosomes and then docked with the SRP on the rough endoplasmic reticulum ▯. The ECD was synthesized and guided into the ER lumen through translocons (channels) to modify and bind unknown protein(s). This binding not only facilitated the retention of the fusion protein but also regulated the oligomerization process to influence the signal transduction of the TM-CT domain. Only the CT oligomer could recruit some proteins to promote vesicle formation ▯. Once the vesicle from ER is formed, gD is transported to the Golgi complex and regains its monomer state in an acidic environment to retain it in the Golgi complex ▯. Vesicle formation was not always inhibited by gD_{EHV-1} in different cells while blocking membrane fusion between induced vesicles and cell membrane was employed to ensure Golgi retention ▯.